

<https://helda.helsinki.fi>

Measurement of an Excess in the Yield of J/psi at Very Low p(T) in Pb-Pb Collisions at $\sqrt{s(NN)}=2.76$ TeV

Adam, J.

2016-06-02

Adam, J, Brucken, E J, Chang, B, Kim, D J, Mieskolainen, M M, Orava, R, Rak, J, Räsänen, S S, Slupecki, M, Snellman, T W, Trzaska, W H, Vargyas, M, Viinikainen, J & The ALICE Collaboration 2016, ' Measurement of an Excess in the Yield of J/psi at Very Low p(T) in Pb-Pb Collisions at $\sqrt{s(NN)}=2.76$ TeV ', Physical Review Letters, vol. 116, no. 22, 222301. <https://doi.org/10.1103/PhysRevLett.116.222301>

<http://hdl.handle.net/10138/165005>

<https://doi.org/10.1103/PhysRevLett.116.222301>

cc_by

publishedVersion

Downloaded from Helda, University of Helsinki institutional repository.

This is an electronic reprint of the original article.

This reprint may differ from the original in pagination and typographic detail.

Please cite the original version.

Measurement of an Excess in the Yield of J/ψ at Very Low p_T in Pb–Pb Collisions at $\sqrt{s_{NN}} = 2.76$ TeV

J. Adam *et al.**

(ALICE Collaboration)

(Received 12 October 2015; published 2 June 2016)

We report on the first measurement of an excess in the yield of J/ψ at very low transverse momentum ($p_T < 0.3$ GeV/ c) in peripheral hadronic Pb-Pb collisions at $\sqrt{s_{NN}} = 2.76$ TeV, performed by ALICE at the CERN LHC. Remarkably, the measured nuclear modification factor of J/ψ in the rapidity range $2.5 < y < 4$ reaches about 7 (2) in the p_T range 0–0.3 GeV/ c in the 70%–90% (50%–70%) centrality class. The J/ψ production cross section associated with the observed excess is obtained under the hypothesis that coherent photoproduction of J/ψ is the underlying physics mechanism. If confirmed, the observation of J/ψ coherent photoproduction in Pb-Pb collisions at impact parameters smaller than twice the nuclear radius opens new theoretical and experimental challenges and opportunities. In particular, coherent photoproduction accompanying hadronic collisions may provide insight into the dynamics of photoproduction and nuclear reactions, as well as become a novel probe of the quark-gluon plasma.

DOI: [10.1103/PhysRevLett.116.222301](https://doi.org/10.1103/PhysRevLett.116.222301)

The aim of experiments with ultrarelativistic heavy-ion collisions is the study of nuclear matter at high temperature and pressure, where quantum chromodynamics (QCD) predicts the existence of a deconfined state of hadronic matter, the quark-gluon plasma (QGP). Heavy quarks are expected to be produced in the primary partonic scatterings and to interact with this partonic matter, making them ideal probes of the QGP. According to the color screening mechanism [1], quarkonium states are suppressed in the QGP, with different dissociation probabilities for the various states depending on the temperature of the medium. On the other hand, regeneration models predict charmonium production via the (re)combination of charm quarks during [2–4] or at the end [5,6] of the deconfined phase. ALICE measurements of the J/ψ nuclear modification factor (R_{AA}) [7–10] and elliptic flow [11] in Pb-Pb collisions at a center-of-mass energy of $\sqrt{s_{NN}} = 2.76$ TeV, as well as the comparison of the J/ψ nuclear modification factor in p -Pb collisions at $\sqrt{s_{NN}} = 5.02$ TeV [12,13] with that in Pb-Pb, support the regeneration scenario.

In this Letter, we report on the measurement of J/ψ production in hadronic Pb-Pb collisions at $\sqrt{s_{NN}} = 2.76$ TeV at very low p_T ($p_T < 0.3$ GeV/ c). We find an excess in the yield of J/ψ with respect to expectations from hadroproduction. A plausible explanation is that the excess is caused by coherent

photoproduction of J/ψ . In this process, quasireal photons coherently produced by the strong electromagnetic field of one of the lead nuclei interact, also coherently, with the gluon field of the other nucleus, to produce a J/ψ . This process proceeds, at leading order in perturbative QCD, through the interchange of two gluons in a singlet color state, probing thus the square of the gluon distribution in the target. The coherence conditions impose a maximum transverse momentum for the produced J/ψ of the order of one over the nuclear radius, so the production occurs at very low p_T . The study of J/ψ photoproduction processes in hadron colliders is known in ultraperipheral collisions (UPCs) and several results are already available in this field at RHIC [14] and at the LHC [15,16]. These measurements give insight into the gluon distribution of the incoming Pb nuclei over a broad range of Bjorken- x values, providing information complementary to the study of J/ψ hadroproduction in p -Pb and Pb-Pb collisions. However, coherent J/ψ photoproduction has never been observed in nuclear collisions with impact parameters smaller than twice the radius of the nuclei. Although the extension to interactions where the nuclei interact hadronically raises several questions, e.g., how the breakup of the nuclei affects the coherence requirement, we find no other convincing explanation. Assuming, therefore, this mechanism causes the observed excess, we obtain the corresponding cross section in the 30%–50%, 50%–70%, and 70%–90% centrality classes.

The ALICE detector is described in Refs. [17,18]. At forward rapidity ($2.5 < y < 4$) the production of quarkonium states is measured via their $\mu^+\mu^-$ decay channel in the muon spectrometer down to $p_T = 0$. The silicon pixel detector (SPD), the scintillator arrays (V0) and the zero degree calorimeters (ZDCs) were also used in this analysis.

*Full author list given at end of the article.

Published by the American Physical Society under the terms of the Creative Commons Attribution 3.0 License. Further distribution of this work must maintain attribution to the author(s) and the published article's title, journal citation, and DOI.

The SPD is located in the central barrel of ALICE, while the V0 and ZDCs are located on both sides of the interaction point. The pseudorapidity coverages of these detectors are $|\eta| < 2$ (first SPD layer), $|\eta| < 1.4$ (second SPD layer), $2.8 < \eta < 5.1$ (V0A), $-3.7 < \eta < -1.7$ (V0C) and $|\eta| > 8.7$ (ZDCs). The SPD provides the coordinates of the primary interaction vertex. The minimum bias (MB) trigger required a signal in the V0 detectors at forward and backward rapidity. In addition to the MB condition, the dimuon opposite-sign trigger ($\mu\mu$ MB), used in this analysis, required at least one pair of opposite-sign track segments detected in the muon spectrometer triggering system, each with a p_T above the 1 GeV/ c threshold of the online trigger algorithm. The background induced by the beam and electromagnetic processes was further reduced by the V0 and ZDCs timing information and by requiring a minimum energy deposited in the two neutron ZDCs (ZNA and ZNC, positioned on opposite sides with respect to the interaction point) [19]. The energy thresholds were ~ 450 GeV for ZNA and ~ 500 GeV for ZNC and were placed approximately 3 standard deviations below the energy deposition of a 1.38 TeV neutron. The data sample used for this analysis amounts to about 17×10^6 $\mu\mu$ MB triggered Pb-Pb collisions, corresponding to an integrated luminosity $\mathcal{L}_{\text{int}} \approx 70 \mu\text{b}^{-1}$. The centrality determination was based on a fit of the V0 amplitude distribution as described in Ref. [20]. A selection corresponding to the 90% most central collisions was applied; for these events the MB trigger was fully efficient. In each centrality class,

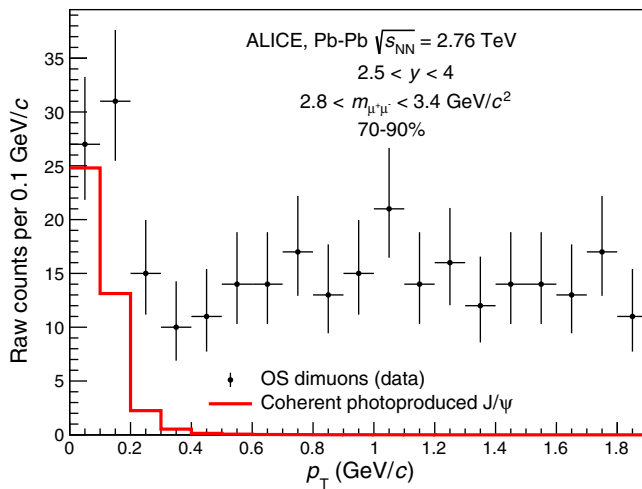


FIG. 1. Raw OS dimuon p_T distribution for the invariant mass range $2.8 < m_{\mu^+\mu^-} < 3.4$ GeV/ c^2 and centrality class 70%–90%. Vertical error bars are the statistical uncertainties. The red line represents the p_T distribution of coherently photoproduced J/ψ as predicted by the STARLIGHT MC generator [22] in Pb-Pb ultraperipheral collisions and convoluted with the response function of the muon spectrometer. The normalization of the red line is given by the measured number of J/ψ in excess reported in Table I after correction for the $\psi(2S)$ feed-down and incoherent contributions (see text).

the average number of participant nucleons $\langle N_{\text{part}} \rangle$ and average value of the nuclear overlap function were derived from a Glauber model calculation [21].

J/ψ candidates were formed by combining pairs of opposite-sign (OS) tracks reconstructed in the geometrical acceptance of the muon spectrometer and matching a track segment above the 1 GeV/ c p_T threshold in the trigger chambers [10]. In Fig. 1, the p_T distribution of OS dimuons, without combinatorial background subtraction, is shown for the invariant mass range $2.8 < m_{\mu^+\mu^-} < 3.4$ GeV/ c^2 in the centrality class 70%–90%. A remarkable excess of dimuons is observed at very low p_T in this centrality class. Such an excess has not been observed in the like-sign dimuon p_T distribution, nor reported in previous measurements in proton-proton collisions [23–28].

The raw number of J/ψ in five centrality classes (0%–10%, 10%–30%, 30%–50%, 50%–70%, and 70%–90%) and three p_T ranges (0–0.3, 0.3–1, 1–8 GeV/ c) was extracted by fitting the OS dimuon invariant mass distribution using a binned likelihood approach. Two functions were considered to describe the J/ψ signal shape: a Crystal Ball function [29] and a pseudo-Gaussian function [30]. The tails of the J/ψ signal

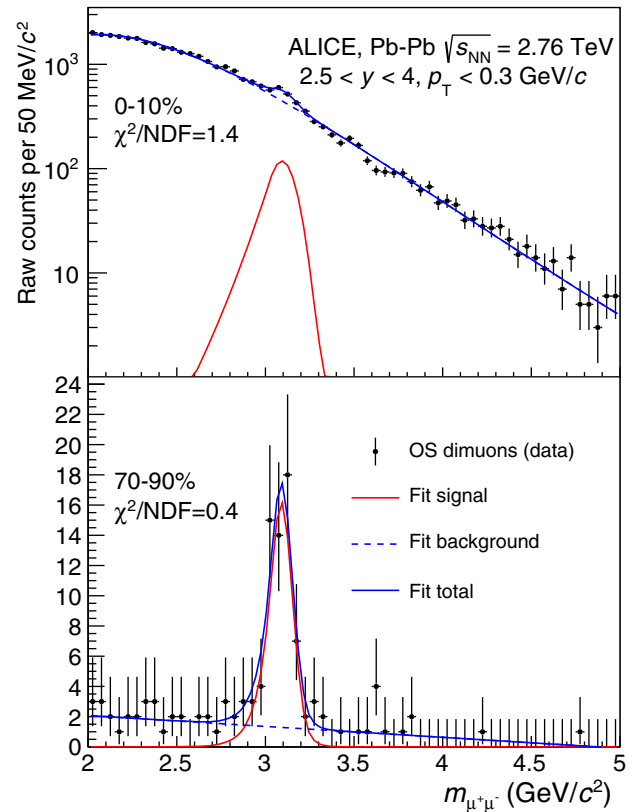


FIG. 2. Invariant mass distributions of OS dimuons in the p_T range 0–0.3 GeV/ c . The centrality classes are 0%–10% (top) and 70%–90% (bottom). Vertical error bars are the statistical uncertainties.

TABLE I. Raw number of J/ψ ($N_{AA}^{J/\psi}$), expected raw number of hadronic J/ψ ($N_{AA}^{hJ/\psi}$), and measured excess in the number of J/ψ ($N_{AA}^{\text{excess}J/\psi}$), all three numbers in the p_T range (0–0.3) GeV/c, and J/ψ coherent photoproduction cross section in Pb-Pb collisions at $\sqrt{s_{NN}} = 2.76$ TeV, with their statistical and uncorrelated systematic uncertainties. A correlated systematic uncertainty also applies to the cross section. In the most central classes, an upper limit (95% C.L.) on the J/ψ yield excess and on the cross section is given.

Cent. (%)	$N_{AA}^{J/\psi}$	$N_{AA}^{hJ/\psi}$	$N_{AA}^{\text{excess}J/\psi}$	$d\sigma_{J/\psi}^{\text{coh}}/dy$ (μb)
0–10	$339 \pm 85 \pm 78$	$406 \pm 14 \pm 55$	< 251	< 318
10–30	$373 \pm 87 \pm 75$	$397 \pm 10 \pm 61$	< 237	< 290
30–50	$187 \pm 37 \pm 15$	$126 \pm 4 \pm 15$	$62 \pm 37 \pm 21$	$73 \pm 44_{-27}^{+26} \pm 10$
50–70	$89 \pm 13 \pm 2$	$39 \pm 2 \pm 5$	$50 \pm 14 \pm 5$	$58 \pm 16_{-10}^{+8} \pm 8$
70–90	$59 \pm 9 \pm 3$	$8 \pm 1 \pm 1$	$51 \pm 9 \pm 3$	$59 \pm 11_{-10}^{+7} \pm 8$

functions were fixed using Monte Carlo (MC) simulations for both hadronic [8] and photoproduction hypotheses [15]. Depending on the p_T range and centrality class under study, two or three functional forms were used to describe the background under the J/ψ signal peak. In addition, the fit range was varied. It has also been checked that changing the invariant mass bin width does not significantly modify the results. Figure 2 shows typical fits in the p_T range 0–0.3 GeV/c for the 0%–10% and 70%–90% centrality classes. The extracted J/ψ signals are the average of the results obtained making all the combinations of signal shapes, background shapes, and fitting ranges, while the systematic uncertainties are given by the rms of the results. The extracted J/ψ signals and the corresponding statistical and systematic uncertainties are quoted in the second column of Table I for the very low p_T range.

In each centrality class and p_T range, the R_{AA} was obtained from the measured number of J/ψ ($N_{AA}^{J/\psi}$) corrected for acceptance and efficiency— $(\mathcal{A} \times \epsilon)_{AA}^{hJ/\psi}$ —(assuming pure hadroproduction with no polarization), branching ratio ($\text{BR}_{J/\psi \rightarrow l^+l^-}$), and normalized to the equivalent number of MB events (N_{events}), average nuclear overlap function ($\langle T_{AA} \rangle$), and proton-proton inclusive J/ψ production cross section ($\sigma_{pp}^{hJ/\psi}$), as detailed in Ref. [8] and shown in Eq. (1):

$$R_{AA}^{hJ/\psi} = \frac{N_{AA}^{J/\psi}}{\text{BR}_{J/\psi \rightarrow l^+l^-} \times N_{\text{events}} \times (\mathcal{A} \times \epsilon)_{AA}^{hJ/\psi} \times \langle T_{AA} \rangle \times \sigma_{pp}^{hJ/\psi}}. \quad (1)$$

In the p_T range 1–8 GeV/c, the J/ψ cross section in pp collisions at $\sqrt{s} = 2.76$ TeV was directly extracted from the ALICE measurement [26], while in the p_T ranges 0–0.3 and 0.3–1 GeV/c, due to limited statistics, it was obtained by fitting the measured p_T distribution with the following parametrization [31]:

$$\frac{d^2\sigma_{pp}^{hJ/\psi}}{dp_T dy} = \frac{c \times \sigma_{J/\psi} \times p_T}{1.5 \times \langle p_T \rangle^2} \left(1 + a^2 \left(\frac{p_T}{\langle p_T \rangle} \right)^2 \right)^{-n}, \quad (2)$$

where $a = \Gamma(3/2)\Gamma(n-3/2)/\Gamma(n-1)$, $c = 2a^2(n-1)$, and $\sigma_{J/\psi}$, $\langle p_T \rangle$ and n are free parameters of the fit. A Lévy-Tsallis function [32,33] and UA1 function [34] were also used to fit the data in order to assess systematic uncertainties. In addition, the validity of the procedure was confirmed using the J/ψ data sample in pp collisions at 7 TeV [23], where the larger statistics at very low p_T allow for a direct measurement of the cross sections: the values obtained with this procedure in the p_T ranges 0–0.3 and 0.3–1 GeV/c agree within 11% (1.2σ) and 4% (0.6σ), respectively, with the measured cross sections.

The procedures for the determination of the various systematic uncertainties are the same as those followed in Ref. [8], apart from the reference pp cross section in the p_T ranges 0–0.3 and 0.3–1 GeV/c, which incorporate the uncertainties of the fitting procedure described above. In Fig. 3, systematic uncertainties were separated into four

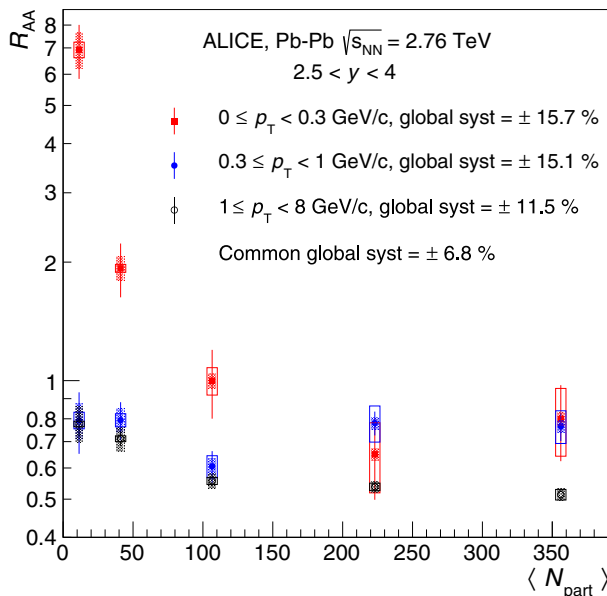


FIG. 3. $J/\psi R_{AA}$ as a function of $\langle N_{\text{part}} \rangle$ for 3 p_T ranges in Pb-Pb collisions at $\sqrt{s_{NN}} = 2.76$ TeV. See text for details on uncertainties. When assuming full transverse polarization of the J/ψ in Pb-Pb collisions, as expected if J/ψ are coherently photoproduced, the R_{AA} values increase by about 21% in the range $0 < p_T < 0.3$ GeV/c.

categories according to their degree of correlation with centrality and p_T : uncorrelated in p_T and centrality (open boxes), which contain the systematic uncertainties of the signal extraction in Pb-Pb (1%–23%); fully correlated as a function of p_T but not as a function of centrality (shaded areas), which contain the uncertainties of the nuclear overlap function (3.2%–7%), of the determination of the centrality classes (0.7%–7.7%), and of the centrality dependence of the tracking (0%–1%) and trigger efficiencies (0%–1%); fully correlated as a function of centrality but not as a function of p_T (quoted as global systematics in the legend), which contain the uncertainties of the J/ψ cross section from pp collisions [statistical (3.6%–6.9%) and uncorrelated systematic (3.2%–8.0%)], of the MC input parametrization (0.5%–2%) and of the tracking (10%–11%), trigger (2.2%–3.6%), and matching efficiencies (1%); and fully correlated in p_T and centrality (quoted as common global systematics), which contain the correlated systematic uncertainty of the pp reference cross section (5.8%) and the uncertainty of the number of equivalent minimum bias events (3.5%).

The $J/\psi R_{AA}$ shown in Fig. 3 exhibits a strong increase in the p_T range 0–0.3 GeV/ c for the most peripheral Pb-Pb collisions. This observation is surprising and none of the transport models [2,3] that well describe the previous measurements [7,8,10] predict such a pattern at LHC energies.

To quantify the excess of J/ψ at very low p_T , we subtracted the number of J/ψ expected from hadroproduction in Pb-Pb collisions. The following parametrization of the number of hadronic J/ψ ($N_{AA}^{hJ/\psi}$) as a function of p_T in a given centrality class was used:

$$\frac{dN_{AA}^{hJ/\psi}}{dp_T} = \mathcal{N} \times \frac{d\sigma_{pp}^{hJ/\psi}}{dp_T} \times R_{AA}^{hJ/\psi} \times (\mathcal{A} \times \epsilon)_{AA}^{hJ/\psi}. \quad (3)$$

The factor \mathcal{N} is fixed by normalizing the integral of Eq. (3) in the p_T range 1–8 GeV/ c to the number of J/ψ measured in the same range, where the hadroproduction component is dominant. The second term is given by the fit of the $J/\psi p_T$ -differential cross section measured in pp collisions [26] using Eq. (2). The third term is a parametrization of the $R_{AA}^{hJ/\psi}$ as a function of p_T from the ALICE measurements in Pb-Pb collisions at 2.76 TeV [8,10]. These measurements are available in three centrality classes (0%–20%, 20%–40%, 40%–90%). To calculate the hadroproduction component in the 10%–30% (30%–50%) centrality class, parameterizations obtained in both 0%–20% and 20%–40% (20%–40% and 40%–90%) were considered. A Woods-Saxon like parametrization, which describes the prediction of transport models on J/ψ production in heavy-ion collisions at low p_T [2,3], was used in all the centrality classes:

$$R_{AA}^{hJ/\psi}(p_T) = R_{AA}^0 + \frac{\Delta R_{AA}}{1 + \exp\left(\frac{p_T - p_T^0}{\sigma_{p_T}}\right)}. \quad (4)$$

R_{AA}^0 , σ_{p_T} , and ΔR_{AA} are free parameters of the fit while the p_T^0 parameter was either unconstrained or fixed to $M_{J/\psi}$ to force an evolution of $R_{AA}^{hJ/\psi}$ at very low p_T in agreement with the predictions of the transport models [2,3]. In addition, a first order polynomial and a constant were used in the most peripheral class. Two fitting ranges in p_T were considered, either 0–8 or 1–8 GeV/ c since the first bin could be biased by the presence of the very low p_T J/ψ excess. Finally, the last term in Eq. (3) is a parametrization of the acceptance times efficiency of hadronic J/ψ [$(\mathcal{A} \times \epsilon)_{AA}^{hJ/\psi}$]—determined from MC simulations of the muon spectrometer response function—with either a third-order polynomial or the ratio of two Lévy–Tsallis functions. Simulations were performed with an embedding technique where MC J/ψ particles are injected into real events and then reconstructed [8]. The results of the various parameterizations are averaged in a given range in p_T and centrality and the rms of the results is included in the systematic uncertainty of the expected number of hadronic J/ψ .

The excess in the number of J/ψ measured in the p_T range 0–0.3 GeV/ c after subtracting the hadronic component is given in the fourth column of Table I. The statistical uncertainty is the quadratic sum of the uncertainties of the measured number of J/ψ in the p_T ranges 0–0.3 and 1–8 GeV/ c . The latter is used in the normalization factor of Eq. (3). The systematic uncertainty is the quadratic sum of the uncertainties of the signal extraction in 0–0.3 GeV/ c (see Table I) and of the parametrization of the hadronic component (13.0%, 12.5%, and 12% in the 70%–90%, 50%–70%, and 30%–50% centrality classes, respectively, see Table I). The significance of the excess is 5.4σ , 3.4σ , and 1.4σ in the 70%–90%, 50%–70%, and 30%–50% centrality classes, respectively. For the two central classes, only the 95% confidence level limit could be computed. To cross-check the robustness of these results, the excess was reevaluated assuming a rough parametrization of the $R_{AA}^{hJ/\psi}$ based on two extreme cases: (i) a constant suppression independent of p_T ($R_{AA}^{hJ/\psi}(p_T < 0.3 \text{ GeV}/c) = R_{AA}^{hJ/\psi}[1 < p_T < 8 \text{ GeV}/c]$), which minimizes the hadronic contribution, and (ii) no suppression at all at low p_T [$R_{AA}^{hJ/\psi}(p_T < 0.3 \text{ GeV}/c) = 1$], which gives the maximum possible hadronic contribution. Even with these simplified and extreme assumptions, the J/ψ excess remains significant and compatible with the results reported in Table I within less than 1 (3) times the quoted systematic uncertainty for the 70%–90% (50%–70%) centrality class.

A plausible explanation of the measured excess is J/ψ photoproduction. The cross section for this process increases with energy and at the LHC becomes comparable to the J/ψ hadronic cross section. Moreover, the shape of the p_T distribution in the region of the observed excess is

similar to that of a coherently photoproduced J/ψ [15], where the photon is emitted by the electromagnetic field of the source nucleus, and then the target nucleus interacts coherently with the photon to produce the J/ψ , like in Pb-Pb ultraperipheral collisions. The average transverse momentum of coherently photoproduced J/ψ is around 0.055 GeV/ c . Detailed MC simulations show that detector effects widen reconstructed distribution by approximately a factor of 2 (see red line in Fig. 1) and that 98% of coherently photoproduced J/ψ are contained in the p_T interval [0, 0.3] GeV/ c .

Assuming that coherent photoproduction causes the excess at very low p_T , the corresponding cross section can be obtained as described in Ref. [15]. The fraction of processes where the coherently emitted photon couples only to a single nucleon, so-called incoherent photoproduction of J/ψ , and passed the data selection is $f_I = 0.14^{+0.16}_{-0.05}$, while the contribution of coherently produced $\psi(2S)$ with a J/ψ among the decay products which passes the data selection is $f_D = 0.10 \pm 0.06$. Both fractions are used to correct the found excess to extract the number of coherent J/ψ . This number was then corrected for the acceptance times efficiency ($\mathcal{A} \times \epsilon = 11.31 \pm 0.04\%$) taking into account that photoproduced J/ψ are expected to be transversally polarized, for the branching ratio, and normalized to the integrated luminosity and the width of the rapidity range. For the 70%–90% centrality class, the cross section per unit of rapidity amounts to $59 \pm 11(\text{stat})_{-10}^{+7}$ (uncor. syst) ± 8 (cor. syst) μb (see Table I, where the values for the other centrality classes are also reported). The uncorrelated centrality dependent systematic uncertainties contain, in addition to the one of the measured excess, the uncertainties of the incoherent and $\psi(2S)$ feed-down contributions (see above), of the determination of the centrality classes (0.7%–7.7%), of the trigger efficiency (0%–1%), of the tracking efficiency (0%–1%), and of the tracking and trigger efficiency loss as a function of centrality (0%–3%). The correlated systematic uncertainties contain the uncertainty of the branching ratio (1%), of the luminosity ($(^{+7.8}_{-6.5}\%)$), of the tracking (11%), trigger (3.6%), and matching efficiencies (1%), and of the MC input parameterization (3%).

In the UPC of lead nuclei at $\sqrt{s_{\text{NN}}} = 2.76$ TeV one expects the incoherent yield in the p_T range 0.3–1 GeV/ c to be about 30% of the coherent yield in the p_T range 0–0.3 GeV/ c [15]. Assuming the same behavior in peripheral collisions, one would expect a 23% (4%) contribution of incoherent J/ψ to the total number of J/ψ measured in the 70%–90% (50%–70%) centrality class in the p_T range 0.3–1 GeV/ c . The significance of the present data sample is not sufficient to confirm the presence of incoherent photoproduction in this p_T range.

The probability of a random coincidence of a MB collision and a coherent production of a J/ψ in a UPC

satisfying the dimuon trigger, in the same bunch crossing, has been evaluated. In the overall data sample, only one random coincidence is expected for the full centrality range, corresponding to 0.6 coincidences in the 30%–90% centrality class.

To our knowledge there is no numerical prediction for the cross section of coherent photoproduction of J/ψ in peripheral collisions. Given that the nuclei also undergo a hadronic interaction, it is not clear how to incorporate the coherence conditions. To have a rough estimate, we considered the extreme assumption that all the charges in the source and all the nucleons in the target contribute to the photonuclear cross section as in coherent UPCs (see also Ref. [35]). The photon flux, see, e.g. Ref. [36], was obtained integrating in the impact parameter range corresponding to the centrality class. We used two different approaches: the vector dominance model of Ref. [37], normalized to the measured UPC data [15,16], and the perturbative QCD model of Ref. [36] with the parameterization of Ref. [38]. In both cases we obtain a cross section in the 70%–90% centrality class of about 40 μb , which is of the same order of magnitude as our measurement. Note that the most peripheral class corresponds to the hadronic interaction of just a few nucleons ($N_{\text{part}} \approx 11$), so the interaction is close to the ultraperipheral case and the comparison to the estimate seems reasonable. Another interesting hypothesis, not considered, would be that only the spectators in the target are the ones that interact coherently with the photon. In this case, the p_T distribution of the excess would get wider as the centrality increases, providing an experimental tool to discriminate among potential models. Indeed, as the size of the spectator region decreases with centrality, the maximum p_T , given by the coherence condition and the uncertainty principle, would increase.

In summary, we reported on the ALICE measurement of J/ψ production at very low p_T and forward rapidity in Pb-Pb collisions at $\sqrt{s_{\text{NN}}} = 2.76$ TeV. A strong increase of the $J/\psi R_{\text{AA}}$ is observed in the range $0 \leq p_T < 0.3$ GeV/ c for the 70%–90% (50%–70%) centrality class, where R_{AA} reaches a value of about 7 (2). The excess has been quantified with a significance of 5.4 (3.4) σ assuming a smooth evolution of the J/ψ hadroproduction at low p_T . Coherent photoproduction of J/ψ is a plausible physics mechanism at the origin of this excess. Following this assumption, the coherent photoproduction cross section has been extracted for the centrality classes 30%–50%, 50%–70%, and 70%–90% while an upper limit is given for 0%–10% and 10%–30%. It would be very challenging for existing theoretical models, which only include hadronic processes, to explain this excess. The survival of an electromagnetically produced charmonium in a nuclear collision merits theoretical investigation. In addition, coherent photoproduced J/ψ may be formed in the initial stage of the collisions and could therefore interact with the QGP,

resulting in a modification of the measured cross section with respect to the expectation of theoretical models. In particular, one expects a partial suppression of photo-produced J/ψ due to color screening of the heavy quark potential in the QGP. The regenerated J/ψ in the QGP exhibit a wider p_T distribution and do not contribute to the measured excess, making this measurement a potentially powerful tool to constrain the suppression or regeneration components in the models. Experimentally, the increase of the LHC heavy ion luminosity during run 2 will lead to a factor 10 larger data sample, thus improving the precision of the present measurement and opening the possibility to determine whether the J/ψ excess at very low p_T is also present in the most central collisions.

The ALICE Collaboration would like to thank all its engineers and technicians for their invaluable contributions to the construction of the experiment and the CERN accelerator teams for the outstanding performance of the LHC complex. The ALICE Collaboration gratefully acknowledges the resources and support provided by all Grid centres and the Worldwide LHC Computing Grid (WLCG) collaboration. The ALICE Collaboration acknowledges the following funding agencies for their support in building and running the ALICE detector: State Committee of Science, World Federation of Scientists (WFS) and Swiss Fonds Kidagan, Armenia; Conselho Nacional de Desenvolvimento Científico e Tecnológico (CNPq), Financiadora de Estudos e Projetos (FINEP), Fundação de Amparo à Pesquisa do Estado de São Paulo (FAPESP); National Natural Science Foundation of China (NSFC), the Chinese Ministry of Education (CMOE) and the Ministry of Science and Technology of China (MSTC); Ministry of Education and Youth of the Czech Republic; Danish Natural Science Research Council, the Carlsberg Foundation and the Danish National Research Foundation; The European Research Council under the European Community's Seventh Framework Programme; Helsinki Institute of Physics and the Academy of Finland; French CNRS-IN2P3, the "Region Pays de Loire," "Region Alsace," "Region Auvergne" and CEA, France; German Bundesministerium für Bildung, Wissenschaft, Forschung und Technologie (BMBF) and the Helmholtz Association; General Secretariat for Research and Technology, Ministry of Development, Greece; Hungarian Országos Tudományos Kutatási Alapprogramok (OTKA) and National Office for Research and Technology (NKTH); Department of Atomic Energy and Department of Science and Technology of the Government of India; Istituto Nazionale di Fisica Nucleare (INFN) and Centro Fermi—Museo Storico della Fisica e Centro Studi e Ricerche "Enrico Fermi", Italy; MEXT Grant-in-Aid for Specially Promoted Research, Japan; Joint Institute for Nuclear Research, Dubna; National Research Foundation of

Korea (NRF); Consejo Nacional de Ciencia y Tecnología (CONACYT), Dirección General de Asuntos del Personal Académico (DGAPA), México, Amérique Latine Formation académique—European Commission (ALFA-EC) and the EPLANET Program (European Particle Physics Latin American Network); Stichting voor Fundamenteel Onderzoek der Materie (FOM) and the Nederlandse Organisatie voor Wetenschappelijk Onderzoek (NWO), Netherlands; Research Council of Norway (NFR); National Science Centre, Poland; Ministry of National Education/Institute for Atomic Physics and National Council of Scientific Research in Higher Education (CNCSI-UEFISCDI), Romania; Ministry of Education and Science of Russian Federation, Russian Academy of Sciences, Russian Federal Agency of Atomic Energy, Russian Federal Agency for Science and Innovations and The Russian Foundation for Basic Research; Ministry of Education of Slovakia; Department of Science and Technology, South Africa; Centro de Investigaciones Energéticas, Medioambientales y Tecnológicas (CIEMAT), E-Infrastructure shared between Europe and Latin America (EELA), Ministerio de Economía y Competitividad (MINECO) of Spain, Xunta de Galicia (Consellería de Educación), Centro de Aplicaciones Tecnológicas y Desarrollo Nuclear (CEADEN), Cubaenergía, Cuba, and IAEA (International Atomic Energy Agency); Swedish Research Council (VR) and Knut & Alice Wallenberg Foundation (KAW); Ukraine Ministry of Education and Science; United Kingdom Science and Technology Facilities Council (STFC); The United States Department of Energy, the United States National Science Foundation, the State of Texas, and the State of Ohio; Ministry of Science, Education and Sports of Croatia and Unity through Knowledge Fund, Croatia; Council of Scientific and Industrial Research (CSIR), New Delhi, India; Pontificia Universidad Católica del Perú.

-
- [1] T. Matsui and H. Satz, J/ψ suppression by quark-gluon plasma formation, *Phys. Lett. B* **178**, 416 (1986).
 - [2] X. Zhao and R. Rapp, Medium modifications and production of charmonia at LHC, *Nucl. Phys. A* **859**, 114 (2011).
 - [3] Y.-P. Liu, Z. Qu, N. Xu, and P.-F. Zhuang, J/ψ transverse momentum distribution in high energy nuclear collisions at RHIC, *Phys. Lett. B* **678**, 72 (2009).
 - [4] R. L. Thews, M. Schroedter, and J. Rafelski, Enhanced J/ψ production in deconfined quark matter, *Phys. Rev. C* **63**, 054905 (2001).
 - [5] P. Braun-Munzinger and J. Stachel, (Non)thermal aspects of charmonium production and a new look at J/ψ suppression, *Phys. Lett. B* **490**, 196 (2000).
 - [6] A. Andronic, P. Braun-Munzinger, K. Redlich, and J. Stachel, The thermal model on the verge of the ultimate test: particle production in Pb-Pb collisions at the LHC, *J. Phys. G* **38**, 124081 (2011).

- [7] B. Abelev *et al.* (ALICE Collaboration), J/ψ Suppression at Forward Rapidity in Pb-Pb Collisions at $\sqrt{s_{NN}} = 2.76$ TeV, *Phys. Rev. Lett.* **109**, 072301 (2012).
- [8] B. Abelev *et al.* (ALICE Collaboration), Centrality, rapidity and transverse momentum dependence of J/ψ suppression in Pb-Pb collisions at $\sqrt{s_{NN}} = 2.76$ TeV, *Phys. Lett. B* **734**, 314 (2014).
- [9] J. Adam *et al.* (ALICE Collaboration), Inclusive, prompt and non-prompt J/ψ production at mid-rapidity in Pb-Pb collisions at $\sqrt{s_{NN}} = 2.76$ TeV, *J. High Energy Phys.* **07** (2015) 051.
- [10] J. Adam *et al.* (ALICE Collaboration), Differential studies of inclusive J/ψ and $\psi(2S)$ production at forward rapidity in Pb-Pb collisions at $\sqrt{s_{NN}} = 2.76$ TeV, [arXiv:1506.08804](https://arxiv.org/abs/1506.08804).
- [11] E. Abbas *et al.* (ALICE Collaboration), J/ψ Elliptic Flow in Pb-Pb Collisions at $\sqrt{s_{NN}} = 2.76$ TeV, *Phys. Rev. Lett.* **111**, 162301 (2013).
- [12] B. Abelev *et al.* (ALICE Collaboration), J/ψ production and nuclear effects in p -Pb collisions at $\sqrt{s_{NN}} = 5.02$ TeV, *J. High Energy Phys.* **02** (2014) 073.
- [13] J. Adam *et al.* (ALICE Collaboration), Rapidity and transverse-momentum dependence of the inclusive J/ψ nuclear modification factor in p -Pb collisions at $\sqrt{s_{NN}} = 5.02$ TeV, *J. High Energy Phys.* **06** (2015) 055.
- [14] S. Afanasiev *et al.* (PHENIX Collaboration), Photoproduction of J/ψ and of high mass e^+e^- in ultra-peripheral Au + Au collisions at $\sqrt{s} = 200$ GeV, *Phys. Lett. B* **679**, 321 (2009).
- [15] B. Abelev *et al.* (ALICE Collaboration), Coherent J/ψ photoproduction in ultra-peripheral Pb-Pb collisions at $\sqrt{s_{NN}} = 2.76$ TeV, *Phys. Lett. B* **718**, 1273 (2013).
- [16] E. Abbas *et al.* (ALICE Collaboration), Charmonium and e^+e^- pair photoproduction at mid-rapidity in ultra-peripheral Pb-Pb collisions at $\sqrt{s_{NN}} = 2.76$ TeV, *Eur. Phys. J. C* **73**, 2617 (2013).
- [17] K. Aamodt *et al.* (ALICE Collaboration), The ALICE experiment at the CERN LHC, *J. Instrum.* **3**, S08002 (2008).
- [18] B. Abelev *et al.* (ALICE Collaboration), Performance of the ALICE experiment at the CERN LHC, *Int. J. Mod. Phys. A* **29**, 1430044 (2014).
- [19] B. Abelev *et al.* (ALICE Collaboration), Measurement of the Cross Section for Electromagnetic Dissociation with Neutron Emission in Pb-Pb Collisions at $\sqrt{s_{NN}} = 2.76$ TeV, *Phys. Rev. Lett.* **109**, 252302 (2012).
- [20] B. Abelev *et al.* (ALICE Collaboration), Centrality determination of Pb-Pb collisions at $\sqrt{s_{NN}} = 2.76$ TeV with ALICE, *Phys. Rev. C* **88**, 044909 (2013).
- [21] M. L. Miller, K. Reygers, S. J. Sanders, and P. Steinberg, Glauber modeling in high energy nuclear collisions, *Annu. Rev. Nucl. Part. Sci.* **57**, 205 (2007).
- [22] STARLIGHT website (2013): <http://starlight.hepforge.org/>.
- [23] B. Abelev *et al.* (ALICE Collaboration), Measurement of quarkonium production at forward rapidity in pp collisions at $\sqrt{s} = 7$ TeV, *Eur. Phys. J. C* **74**, 2974 (2014).
- [24] K. Aamodt *et al.* (ALICE Collaboration), Rapidity and transverse momentum dependence of inclusive J/ψ production in pp collisions at $\sqrt{s} = 7$ TeV, *Phys. Lett. B* **704**, 442 (2011).
- [25] B. Abelev *et al.* (ALICE Collaboration), J/ψ Production as a Function of Charged Particle Multiplicity in pp Collisions at $\sqrt{s} = 7$ TeV, *Phys. Lett. B* **712**, 165 (2012).
- [26] B. Abelev *et al.* (ALICE Collaboration), Inclusive J/ψ production in pp collisions at $\sqrt{s} = 2.76$ TeV, *Phys. Lett. B* **718**, 295 (2012).
- [27] R. Aaij *et al.* (LHCb Collaboration), Measurement of J/ψ production in pp collisions at $\sqrt{s} = 7$ TeV, *Eur. Phys. J. C* **71**, 1645 (2011).
- [28] R. Aaij *et al.* (LHCb Collaboration), Measurement of J/ψ production in pp collisions at $\sqrt{s} = 2.76$ TeV, *J. High Energy Phys.* **02** (2013) 041.
- [29] J. E. Gaiser, Ph.D. thesis, Stanford, 1982. Appendix-F, SLAC-R-255.
- [30] R. Shahoyan, Ph.D. thesis, Instituto Superior Técnico, Universidade Tecnica de Lisboa, 2001.
- [31] F. Bossu *et al.*, Phenomenological extrapolation of the inclusive J/ψ cross section to proton-proton collisions at 2.76 TeV and 5.5 TeV, [arXiv:1103.2394](https://arxiv.org/abs/1103.2394).
- [32] C. Tsallis, Possible generalization of Boltzmann-Gibbs statistics, *J. Stat. Phys.* **52**, 479 (1988).
- [33] B. Abelev *et al.* (STAR Collaboration), Strange particle production in $p + p$ collisions at $\sqrt{s} = 200$ GeV, *Phys. Rev. C* **75**, 064901 (2007).
- [34] C. Albajar *et al.* (UA1 Collaboration), A study of the general characteristics of $p\bar{p}$ collisions at $\sqrt{s} = 0.2$ TeV to 0.9 TeV, *Nucl. Phys.* **B335**, 261 (1990).
- [35] M. Kusek-Gawenda and A. Szczurek, Photoproduction of J/ψ mesons in peripheral and semi-central heavy ion collisions, [arXiv:1509.03173](https://arxiv.org/abs/1509.03173).
- [36] G. Baur, K. Hencken, D. Trautmann, S. Sadovsky, and Y. Kharlov, Coherent $\gamma\gamma$ and γA interactions in very peripheral collisions at relativistic ion colliders, *Phys. Rep.* **364**, 359 (2002).
- [37] S. Klein and J. Nystrand, Exclusive vector meson production in relativistic heavy ion collisions, *Phys. Rev. C* **60**, 014903 (1999).
- [38] V. Guzey, E. Kryshen, M. Strikman, and M. Zhalov, Evidence for nuclear gluon shadowing from the ALICE measurements of PbPb ultraperipheral exclusive J/ψ production, *Phys. Lett. B* **726**, 290 (2013).

J. Adam,⁴⁰ D. Adamová,⁸⁴ M. M. Aggarwal,⁸⁸ G. Aglieri Rinella,³⁶ M. Agnello,¹¹⁰ N. Agrawal,⁴⁸ Z. Ahammed,¹³² S. U. Ahn,⁶⁸ S. Aiola,¹³⁶ A. Akindinov,⁵⁸ S. N. Alam,¹³² D. Aleksandrov,⁸⁰ B. Alessandro,¹¹⁰ D. Alexandre,¹⁰¹ R. Alfaro Molina,⁶⁴ A. Alici,^{12,104} A. Alkin,³ J. R. M. Almaraz,¹¹⁹ J. Alme,³⁸ T. Alt,⁴³ S. Altinpinar,¹⁸ I. Altsybeev,¹³¹ C. Alves Garcia Prado,¹²⁰ C. Andrei,⁷⁸ A. Andronic,⁹⁷ V. Anguelov,⁹⁴ J. Anielski,⁵⁴ T. Antičić,⁹⁸ F. Antinori,¹⁰⁷ P. Antonioli,¹⁰⁴ L. Aphecetche,¹¹³ H. Appelshäuser,⁵³ S. Arcelli,²⁸ R. Arnaldi,¹¹⁰ O. W. Arnold,^{37,93} I. C. Arsene,²²

M. Arslandok,⁵³ B. Audurier,¹¹³ A. Augustinus,³⁶ R. Averbeck,⁹⁷ M. D. Azmi,¹⁹ A. Badalà,¹⁰⁶ Y. W. Baek,⁶⁷ S. Bagnasco,¹¹⁰ R. Bailhache,⁵³ R. Bala,⁹¹ A. Baldisseri,¹⁵ R. C. Baral,⁶¹ A. M. Barbano,²⁷ R. Barbera,²⁹ F. Barile,³³ G. G. Barnaföldi,¹³⁵ L. S. Barnby,¹⁰¹ V. Barret,⁷⁰ P. Bartalini,⁷ K. Barth,³⁶ J. Bartke,¹¹⁷ E. Bartsch,⁵³ M. Basile,²⁸ N. Bastid,⁷⁰ S. Basu,¹³² B. Bathen,⁵⁴ G. Batigne,¹¹³ A. Batista Camejo,⁷⁰ B. Batyunya,⁶⁶ P. C. Batzing,²² I. G. Bearden,⁸¹ H. Beck,⁵³ C. Bedda,¹¹⁰ N. K. Behera,⁵⁰ I. Belikov,⁵⁵ F. Bellini,²⁸ H. Bello Martinez,² R. Bellwied,¹²² R. Belmont,¹³⁴ E. Belmont-Moreno,⁶⁴ V. Belyaev,⁷⁵ G. Bencedi,¹³⁵ S. Beole,²⁷ I. Berceanu,⁷⁸ A. Bercuci,⁷⁸ Y. Berdnikov,⁸⁶ D. Berenyi,¹³⁵ R. A. Bertens,⁵⁷ D. Berzano,³⁶ L. Betev,³⁶ A. Bhasin,⁹¹ I. R. Bhat,⁹¹ A. K. Bhati,⁸⁸ B. Bhattacharjee,⁴⁵ J. Bhom,¹²⁸ L. Bianchi,¹²² N. Bianchi,⁷² C. Bianchin,^{57,134} J. Bielčák,⁴⁰ J. Bielčáková,⁸⁴ A. Bilandzic,⁸¹ R. Biswas,⁴ S. Biswas,⁷⁹ S. Bjelogrić,⁵⁷ J. T. Blair,¹¹⁸ D. Blau,⁸⁰ C. Blume,⁵³ F. Bock,^{94,74} A. Bogdanov,⁷⁵ H. Bøggild,⁸¹ L. Boldizsár,¹³⁵ M. Bombara,⁴¹ J. Book,⁵³ H. Borel,¹⁵ A. Borissov,⁹⁶ M. Borri,^{83,124} F. Bossú,⁶⁵ E. Botta,²⁷ S. Böttger,⁵² C. Bourjau,⁸¹ P. Braun-Munzinger,⁹⁷ M. Bregant,¹²⁰ T. Breitner,⁵² T. A. Broker,⁵³ T. A. Browning,⁹⁵ M. Broz,⁴⁰ E. J. Brucken,⁴⁶ E. Bruna,¹¹⁰ G. E. Bruno,³³ D. Budnikov,⁹⁹ H. Buesching,⁵³ S. Bufalino,^{27,36} P. Buncic,³⁶ O. Busch,^{94,128} Z. Buthelezi,⁶⁵ J. B. Butt,¹⁶ J. T. Buxton,²⁰ D. Caffarri,³⁶ X. Cai,⁷ H. Caines,¹³⁶ L. Calero Diaz,⁷² A. Caliva,⁵⁷ E. Calvo Villar,¹⁰² P. Camerini,²⁶ F. Carena,³⁶ W. Carena,³⁶ F. Carnesecchi,²⁸ J. Castillo Castellanos,¹⁵ A. J. Castro,¹²⁵ E. A. R. Casula,²⁵ C. Ceballos Sanchez,⁹ J. Cepila,⁴⁰ P. Cerello,¹¹⁰ J. Cerkala,¹¹⁵ B. Chang,¹²³ S. Chapeland,³⁶ M. Chartier,¹²⁴ J. L. Charvet,¹⁵ S. Chattopadhyay,¹³² S. Chattopadhyay,¹⁰⁰ V. Chelnokov,³ M. Cherney,⁸⁷ C. Cheshkov,¹³⁰ B. Cheynis,¹³⁰ V. Chibante Barroso,³⁶ D. D. Chinellato,¹²¹ S. Cho,⁵⁰ P. Chochula,³⁶ K. Choi,⁹⁶ M. Chojnacki,⁸¹ S. Choudhury,¹³² P. Christakoglou,⁸² C. H. Christensen,⁸¹ P. Christiansen,³⁴ T. Chujo,¹²⁸ S. U. Chung,⁹⁶ C. Cicalo,¹⁰⁵ L. Cifarelli,^{12,28} F. Cindolo,¹⁰⁴ J. Cleymans,⁹⁰ F. Colamaria,³³ D. Colella,^{59,33,36} A. Collu,^{74,25} M. Colocci,²⁸ G. Conesa Balbastre,⁷¹ Z. Conesa del Valle,⁵¹ M. E. Connors,^{136,a} J. G. Contreras,⁴⁰ T. M. Cormier,⁸⁵ Y. Corrales Morales,¹¹⁰ I. Cortés Maldonado,² P. Cortese,³² M. R. Cosentino,¹²⁰ F. Costa,³⁶ P. Crochet,⁷⁰ R. Cruz Albino,¹¹ E. Cuautele,⁶³ L. Cunqueiro,³⁶ T. Dahms,^{93,37} A. Dainese,¹⁰⁷ A. Danu,⁶² D. Das,¹⁰⁰ I. Das,^{51,100} S. Das,⁴ A. Dash,^{121,79} S. Dash,⁴⁸ S. De,¹²⁰ A. De Caro,^{31,12} G. de Cataldo,¹⁰³ C. de Conti,¹²⁰ J. de Cuveland,⁴³ A. De Falco,²⁵ D. De Gruttola,^{12,31} N. De Marco,¹¹⁰ S. De Pasquale,³¹ A. Deisting,^{97,94} A. Deloff,⁷⁷ E. Dénes,^{135,†} C. Deplano,⁸² P. Dhankher,⁴⁸ D. Di Bari,³³ A. Di Mauro,³⁶ P. Di Nezza,⁷² M. A. Diaz Corchero,¹⁰ T. Dietel,⁹⁰ P. Dillenseger,⁵³ R. Divià,³⁶ Ø. Djuvsland,¹⁸ A. Dobrin,^{57,82} D. Domenicis Gimenez,¹²⁰ B. Dönigus,⁵³ O. Dordic,²² T. Drozhzhova,⁵³ A. K. Dubey,¹³² A. Dubla,⁵⁷ L. Ducroux,¹³⁰ P. Dupieux,⁷⁰ R. J. Ehlers,¹³⁶ D. Elia,¹⁰³ H. Engel,⁵² E. Eppe,¹³⁶ B. Erasmus,¹¹³ I. Erdemir,⁵³ F. Erhardt,¹²⁹ B. Espagnon,⁵¹ M. Estienne,¹¹³ S. Esumi,¹²⁸ J. Eum,⁹⁶ D. Evans,¹⁰¹ S. Evdokimov,¹¹¹ G. Eyyubova,⁴⁰ L. Fabbietti,^{93,37} D. Fabris,¹⁰⁷ J. Faivre,⁷¹ A. Fantoni,⁷² M. Fasel,⁷⁴ L. Feldkamp,⁵⁴ A. Feliciello,¹¹⁰ G. Feofilov,¹³¹ J. Ferencei,⁸⁴ A. Fernández Téllez,² E. G. Ferreira,¹⁷ A. Ferretti,²⁷ A. Festanti,³⁰ V. J. G. Feuillard,^{15,70} J. Figiel,¹¹⁷ M. A. S. Figueredo,^{124,120} S. Filchagin,⁹⁹ D. Finogeev,⁵⁶ F. M. Fionda,²⁵ E. M. Fiore,³³ M. G. Fleck,⁹⁴ M. Floris,³⁶ S. Foertsch,⁶⁵ P. Foka,⁹⁷ S. Fokin,⁸⁰ E. Fragiaco,¹⁰⁹ A. Francescon,^{30,36} U. Frankenfeld,⁹⁷ U. Fuchs,³⁶ C. Furget,⁷¹ A. Furs,⁵⁶ M. Fusco Girard,³¹ J. J. Gaardhøje,⁸¹ M. Gagliardi,²⁷ A. M. Gago,¹⁰² M. Gallio,²⁷ D. R. Gangadharan,⁷⁴ P. Ganoti,^{36,89} C. Gao,⁷ C. Garabatos,⁹⁷ E. Garcia-Solis,¹³ C. Gargiulo,³⁶ P. Gasik,^{37,93} E. F. Gauger,¹¹⁸ M. Germain,¹¹³ A. Gheata,³⁶ M. Gheata,^{62,36} P. Ghosh,¹³² S. K. Ghosh,⁴ P. Gianotti,⁷² P. Giubellino,^{110,36} P. Giubilato,³⁰ E. Gladysz-Dziadus,¹¹⁷ P. Glässel,⁹⁴ D. M. Gómez Coral,⁶⁴ A. Gomez Ramirez,⁵² V. Gonzalez,¹⁰ P. González-Zamora,¹⁰ S. Gorbunov,⁴³ L. Görlich,¹¹⁷ S. Gotovac,¹¹⁶ V. Grabski,⁶⁴ O. A. Grachov,¹³⁶ L. K. Graczykowski,¹³³ K. L. Graham,¹⁰¹ A. Grelli,⁵⁷ A. Grigoras,³⁶ C. Grigoras,³⁶ V. Grigoriev,⁷⁵ A. Grigoryan,¹ S. Grigoryan,⁶⁶ B. Grinyov,³ N. Grion,¹⁰⁹ J. M. Gronefeld,⁹⁷ J. F. Grosse-Oetringhaus,³⁶ J.-Y. Grossiord,¹³⁰ R. Grosso,⁹⁷ F. Guber,⁵⁶ R. Guernane,⁷¹ B. Guerzoni,²⁸ K. Gulbrandsen,⁸¹ T. Gunji,¹²⁷ A. Gupta,⁹¹ R. Gupta,⁹¹ R. Haake,⁵⁴ Ø. Haaland,¹⁸ C. Hadjidakis,⁵¹ M. Haiduc,⁶² H. Hamagaki,¹²⁷ G. Hamar,¹³⁵ J. W. Harris,¹³⁶ A. Harton,¹³ D. Hatzifotiadiou,¹⁰⁴ S. Hayashi,¹²⁷ S. T. Heckel,⁵³ M. Heide,⁵⁴ H. Helstrup,³⁸ A. Herghelegiu,⁷⁸ G. Herrera Corral,¹¹ B. A. Hess,³⁵ K. F. Hetland,³⁸ H. Hillemanns,³⁶ B. Hippolyte,⁵⁵ R. Hosokawa,¹²⁸ P. Hristov,³⁶ M. Huang,¹⁸ T. J. Humanic,²⁰ N. Hussain,⁴⁵ T. Hussain,¹⁹ D. Hutter,⁴³ D. S. Hwang,²¹ R. Ilkaev,⁹⁹ M. Inaba,¹²⁸ M. Ippolitov,^{75,80} M. Irfan,¹⁹ M. Ivanov,⁹⁷ V. Ivanov,⁸⁶ V. Izucheev,¹¹¹ P. M. Jacobs,⁷⁴ M. B. Jadhav,⁴⁸ S. Jadlovska,¹¹⁵ J. Jadlovsky,^{115,59} C. Jahnke,¹²⁰ M. J. Jakubowska,¹³³ H. J. Jang,⁶⁸ M. A. Janik,¹³³ P. H. S. Y. Jayarathna,¹²² C. Jena,³⁰ S. Jena,¹²² R. T. Jimenez Bustamante,⁹⁷ P. G. Jones,¹⁰¹ H. Jung,⁴⁴ A. Jusko,¹⁰¹ P. Kalinak,⁵⁹ A. Kalweit,³⁶ J. Kamin,⁵³ J. H. Kang,¹³⁷ V. Kaplin,⁷⁵ S. Kar,¹³² A. Karasu Uysal,⁶⁹ O. Karavichev,⁵⁶ T. Karavicheva,⁵⁶ L. Karayan,^{97,94} E. Karpechev,⁵⁶ U. Kebschull,⁵² R. Keidel,¹³⁸ D. L. D. Keijdener,⁵⁷ M. Keil,³⁶ M. Mohisin Khan,^{19,b} P. Khan,¹⁰⁰ S. A. Khan,¹³² A. Khanzadeev,⁸⁶ Y. Kharlov,¹¹¹ B. Kileng,³⁸ D. W. Kim,⁴⁴ D. J. Kim,¹²³ D. Kim,¹³⁷ H. Kim,¹³⁷ J. S. Kim,⁴⁴ M. Kim,⁴⁴ M. Kim,¹³⁷ S. Kim,²¹ T. Kim,¹³⁷ S. Kirsch,⁴³ I. Kisel,⁴³

S. Kiselev,⁵⁸ A. Kisiel,¹³³ G. Kiss,¹³⁵ J. L. Klay,⁶ C. Klein,⁵³ J. Klein,^{36,94} C. Klein-Bösing,⁵⁴ S. Klewin,⁹⁴ A. Kluge,³⁶ M. L. Knichel,⁹⁴ A. G. Knospe,¹¹⁸ T. Kobayashi,¹²⁸ C. Kobdaj,¹¹⁴ M. Kofarago,³⁶ T. Kollegger,^{97,43} A. Kolojvari,¹³¹ V. Kondratiev,¹³¹ N. Kondratyeva,⁷⁵ E. Kondratyuk,¹¹¹ A. Konevskikh,⁵⁶ M. Kopcik,¹¹⁵ M. Kour,⁹¹ C. Kouzinopoulos,³⁶ O. Kovalenko,⁷⁷ V. Kovalenko,¹³¹ M. Kowalski,¹¹⁷ G. Koyithatta Meethalevedu,⁴⁸ I. Králik,⁵⁹ A. Kravčáková,⁴¹ M. Kretz,⁴³ M. Krivda,^{101,59} F. Krizek,⁸⁴ E. Kryshen,³⁶ M. Krzewicki,⁴³ A. M. Kubera,²⁰ V. Kučera,⁸⁴ C. Kuhn,⁵⁵ P. G. Kuijjer,⁸² A. Kumar,⁹¹ J. Kumar,⁴⁸ L. Kumar,⁸⁸ S. Kumar,⁴⁸ P. Kurashvili,⁷⁷ A. Kurepin,⁵⁶ A. B. Kurepin,⁵⁶ A. Kuryakin,⁹⁹ M. J. Kweon,⁵⁰ Y. Kwon,¹³⁷ S. L. La Pointe,¹¹⁰ P. La Rocca,²⁹ P. Ladron de Guevara,¹¹ C. Lagana Fernandes,¹²⁰ I. Lakomov,³⁶ R. Langoy,⁴² C. Lara,⁵² A. Lardeux,¹⁵ A. Lattuca,²⁷ E. Laudi,³⁶ R. Lea,²⁶ L. Leardini,⁹⁴ G. R. Lee,¹⁰¹ S. Lee,¹³⁷ F. Lehas,⁸² R. C. Lemmon,⁸³ V. Lenti,¹⁰³ E. Leogrande,⁵⁷ I. León Monzón,¹¹⁹ H. León Vargas,⁶⁴ M. Leoncino,²⁷ P. Lévai,¹³⁵ S. Li,^{70,7} X. Li,¹⁴ J. Lien,⁴² R. Lietava,¹⁰¹ S. Lindal,²² V. Lindenstruth,⁴³ C. Lippmann,⁹⁷ M. A. Lisa,²⁰ H. M. Ljunggren,³⁴ D. F. Lodato,⁵⁷ P. I. Loenne,¹⁸ V. Loginov,⁷⁵ C. Loizides,⁷⁴ X. Lopez,⁷⁰ E. López Torres,⁹ A. Lowe,¹³⁵ P. Luetig,⁵³ M. Lunardon,³⁰ G. Luparello,²⁶ A. Maevskaya,⁵⁶ M. Mager,³⁶ S. Mahajan,⁹¹ S. M. Mahmood,²² A. Maire,⁵⁵ R. D. Majka,¹³⁶ M. Malaev,⁸⁶ I. Maldonado Cervantes,⁶³ L. Malinina,^{66,c} D. Mal'Kevich,⁵⁸ P. Malzacher,⁹⁷ A. Mamonov,⁹⁹ V. Manko,⁸⁰ F. Manso,⁷⁰ V. Manzari,^{36,103} M. Marchisone,^{126,27,65} J. Mareš,⁶⁰ G. V. Margagliotti,²⁶ A. Margotti,¹⁰⁴ J. Margutti,⁵⁷ A. Marín,⁹⁷ C. Markert,¹¹⁸ M. Marquard,⁵³ N. A. Martin,⁹⁷ J. Martin Blanco,¹¹³ P. Martinengo,³⁶ M. I. Martínez,² G. Martínez García,¹¹³ M. Martinez Pedreira,³⁶ A. Mas,¹²⁰ S. Masciocchi,⁹⁷ M. Maserà,²⁷ A. Masoni,¹⁰⁵ L. Massacrier,¹¹³ A. Mastroserio,³³ A. Matyja,¹¹⁷ C. Mayer,¹¹⁷ J. Mazer,¹²⁵ M. A. Mazzoni,¹⁰⁸ D. McDonald,¹²² F. Meddi,²⁴ Y. Melikyan,⁷⁵ A. Menchaca-Rocha,⁶⁴ E. Meninno,³¹ J. Mercado Pérez,⁹⁴ M. Meres,³⁹ Y. Miake,¹²⁸ M. M. Mieskolainen,⁴⁶ K. Mikhaylov,^{58,66} L. Milano,^{36,74} J. Milosevic,²² L. M. Minervini,^{103,23} A. Mischke,⁵⁷ A. N. Mishra,⁴⁹ D. Miśkowiec,⁹⁷ J. Mitra,¹³² C. M. Mitu,⁶² N. Mohammadi,⁵⁷ B. Mohanty,^{132,79} L. Molnar,^{113,55} L. Montaña Zetina,¹¹ E. Montes,¹⁰ D. A. Moreira De Godoy,^{113,54} L. A. P. Moreno,² S. Moretto,³⁰ A. Morreale,¹¹³ A. Morsch,³⁶ V. Muccifora,⁷² E. Mudnic,¹¹⁶ D. Mühlheim,⁵⁴ S. Muhuri,¹³² M. Mukherjee,¹³² J. D. Mulligan,¹³⁶ M. G. Munhoz,¹²⁰ R. H. Munzer,^{37,93} S. Murray,⁶⁵ L. Musa,³⁶ J. Musinsky,⁵⁹ B. Naik,⁴⁸ R. Nair,⁷⁷ B. K. Nandi,⁴⁸ R. Nania,¹⁰⁴ E. Nappi,¹⁰³ M. U. Naru,¹⁶ H. Natal da Luz,¹²⁰ C. Nattrass,¹²⁵ K. Nayak,⁷⁹ T. K. Nayak,¹³² S. Nazarenko,⁹⁹ A. Nedosekin,⁵⁸ L. Nellen,⁶³ F. Ng,¹²² M. Nicassio,⁹⁷ M. Niculescu,⁶² J. Niedziela,³⁶ B. S. Nielsen,⁸¹ S. Nikolaev,⁸⁰ S. Nikulin,⁸⁰ V. Nikulin,⁸⁶ F. Noferini,^{12,104} P. Nomokonov,⁶⁶ G. Nooren,⁵⁷ J. C. C. Noris,² J. Norman,¹²⁴ A. Nyanin,⁸⁰ J. Nystrand,¹⁸ H. Oeschler,⁹⁴ S. Oh,¹³⁶ S. K. Oh,⁶⁷ A. Ohlson,³⁶ A. Okatan,⁶⁹ T. Okubo,⁴⁷ L. Olah,¹³⁵ J. Oleniacz,¹³³ A. C. Oliveira Da Silva,¹²⁰ M. H. Oliver,¹³⁶ J. Onderwaater,⁹⁷ C. Oppedisano,¹¹⁰ R. Orava,⁴⁶ A. Ortiz Velasquez,⁶³ A. Oskarsson,³⁴ J. Otwinowski,¹¹⁷ K. Oyama,^{94,76} M. Ozdemir,⁵³ Y. Pachmayer,⁹⁴ P. Pagano,³¹ G. Paić,⁶³ S. K. Pal,¹³² J. Pan,¹³⁴ A. K. Pandey,⁴⁸ P. Papcun,¹¹⁵ V. Papikyan,¹ G. S. Pappalardo,¹⁰⁶ P. Pareek,⁴⁹ W. J. Park,⁹⁷ S. Parmar,⁸⁸ A. Passfeld,⁵⁴ V. Patricchio,¹⁰³ R. N. Patra,¹³² B. Paul,¹⁰⁰ H. Pei,⁷ T. Peitzmann,⁵⁷ H. Pereira Da Costa,¹⁵ E. Pereira De Oliveira Filho,¹²⁰ D. Peresunko,^{80,75} C. E. Pérez Lara,⁸² E. Perez Lezama,⁵³ V. Peskov,⁵³ Y. Pestov,⁵ V. Petráček,⁴⁰ V. Petrov,¹¹¹ M. Petrovici,⁷⁸ C. Petta,²⁹ S. Piano,¹⁰⁹ M. Pikna,³⁹ P. Pillot,¹¹³ O. Pinazza,^{104,36} L. Pinsky,¹²² D. B. Piyarathna,¹²² M. Płoskoń,⁷⁴ M. Planinic,¹²⁹ J. Pluta,¹³³ S. Pochybova,¹³⁵ P. L. M. Podesta-Lerma,¹¹⁹ M. G. Poghosyan,^{85,87} B. Polichtchouk,¹¹¹ N. Poljak,¹²⁹ W. Poonsawat,¹¹⁴ A. Pop,⁷⁸ S. Porteboeuf-Houssais,⁷⁰ J. Porter,⁷⁴ J. Pospisil,⁸⁴ S. K. Prasad,⁴ R. Preghenella,^{104,36} F. Prino,¹¹⁰ C. A. Pruneau,¹³⁴ I. Pshenichnov,⁵⁶ M. Puccio,²⁷ G. Puddu,²⁵ P. Pujahari,¹³⁴ V. Punin,⁹⁹ J. Putschke,¹³⁴ H. Qvigstad,²² A. Rachevski,¹⁰⁹ S. Raha,⁴ S. Rajput,⁹¹ J. Rak,¹²³ A. Rakotozafindrabe,¹⁵ L. Ramello,³² F. Rami,⁵⁵ R. Raniwala,⁹² S. Raniwala,⁹² S. S. Räsänen,⁴⁶ B. T. Rascanu,⁵³ D. Rathee,⁸⁸ K. F. Read,^{125,85} K. Redlich,⁷⁷ R. J. Reed,¹³⁴ A. Rehman,¹⁸ P. Reichelt,⁵³ F. Reidt,^{94,36} X. Ren,⁷ R. Renfordt,⁵³ A. R. Reolon,⁷² A. Reshetin,⁵⁶ J.-P. Revol,¹² K. Reygers,⁹⁴ V. Riabov,⁸⁶ R. A. Ricci,⁷³ T. Richert,³⁴ M. Richter,²² P. Riedler,³⁶ W. Riegler,³⁶ F. Riggi,²⁹ C. Ristea,⁶² E. Rocco,⁵⁷ M. Rodríguez Cahuantzi,^{2,11} A. Rodríguez Manso,⁸² K. Røed,²² E. Rogochaya,⁶⁶ D. Rohr,⁴³ D. Röhrich,¹⁸ R. Romita,¹²⁴ F. Ronchetti,^{72,36} L. Ronflette,¹¹³ P. Rosnet,⁷⁰ A. Rossi,^{30,36} F. Roukoutakis,⁸⁹ A. Roy,⁴⁹ C. Roy,⁵⁵ P. Roy,¹⁰⁰ A. J. Rubio Montero,¹⁰ R. Rui,²⁶ R. Russo,²⁷ E. Ryabinkin,⁸⁰ Y. Ryabov,⁸⁶ A. Rybicki,¹¹⁷ S. Sadovsky,¹¹¹ K. Šafařík,³⁶ B. Sahlmuller,⁵³ P. Sahoo,⁴⁹ R. Sahoo,⁴⁹ S. Sahoo,⁶¹ P. K. Sahu,⁶¹ J. Saini,¹³² S. Sakai,⁷² M. A. Saleh,¹³⁴ J. Salzwedel,²⁰ S. Sambyal,⁹¹ V. Samsonov,⁸⁶ L. Šándor,⁵⁹ A. Sandoval,⁶⁴ M. Sano,¹²⁸ D. Sarkar,¹³² E. Scapparone,¹⁰⁴ F. Scarlassara,³⁰ C. Schiaua,⁷⁸ R. Schicker,⁹⁴ C. Schmidt,⁹⁷ H. R. Schmidt,³⁵ S. Schuchmann,⁵³ J. Schukraft,³⁶ M. Schulc,⁴⁰ T. Schuster,¹³⁶ Y. Schutz,^{36,113} K. Schwarz,⁹⁷ K. Schweda,⁹⁷ G. Scioli,²⁸ E. Scomparin,¹¹⁰ R. Scott,¹²⁵ M. Šefčík,⁴¹ J. E. Seger,⁸⁷ Y. Sekiguchi,¹²⁷ D. Sekihata,⁴⁷ I. Selyuzhenkov,⁹⁷ K. Senosi,⁶⁵ S. Senyukov,^{3,36} E. Serradilla,^{10,64} A. Sevcenco,⁶² A. Shabanov,⁵⁶ A. Shabetai,¹¹³ O. Shadura,³ R. Shahoyan,³⁶

A. Shangaraev,¹¹¹ A. Sharma,⁹¹ M. Sharma,⁹¹ M. Sharma,⁹¹ N. Sharma,¹²⁵ K. Shigaki,⁴⁷ K. Shtejer,^{9,27} Y. Sibiriak,⁸⁰ S. Siddhanta,¹⁰⁵ K. M. Sielewicz,³⁶ T. Siemiarczuk,⁷⁷ D. Silvermyr,^{34,85} C. Silvestre,⁷¹ G. Simatovic,¹²⁹ G. Simonetti,³⁶ R. Singaraju,¹³² R. Singh,⁷⁹ S. Singha,^{79,132} V. Singhal,¹³² B. C. Sinha,¹³² T. Sinha,¹⁰⁰ B. Sitar,³⁹ M. Sitta,³² T. B. Skaali,²² M. Slupecki,¹²³ N. Smirnov,¹³⁶ R. J. M. Snellings,⁵⁷ T. W. Snellman,¹²³ C. Sogaard,³⁴ J. Song,⁹⁶ M. Song,¹³⁷ Z. Song,⁷ F. Soramel,³⁰ S. Sorensen,¹²⁵ F. Sozzi,⁹⁷ M. Spacek,⁴⁰ E. Spiriti,⁷² I. Sputowska,¹¹⁷ M. Spyropoulou-Stassinaki,⁸⁹ J. Stachel,⁹⁴ I. Stan,⁶² G. Stefanek,⁷⁷ E. Stenlund,³⁴ G. Steyn,⁶⁵ J. H. Stiller,⁹⁴ D. Stocco,¹¹³ P. Strmen,³⁹ A. A. P. Suaide,¹²⁰ T. Sugitate,⁴⁷ C. Suire,⁵¹ M. Suleymanov,¹⁶ M. Suljic,^{26,†} R. Sultanov,⁵⁸ M. Šumbera,⁸⁴ A. Szabo,³⁹ A. Szanto de Toledo,^{120,†} I. Szarka,³⁹ A. Szczepankiewicz,³⁶ M. Szymanski,¹³³ U. Tabassam,¹⁶ J. Takahashi,¹²¹ G. J. Tambave,¹⁸ N. Tanaka,¹²⁸ M. A. Tangaro,³³ M. Tarhini,⁵¹ M. Tariq,¹⁹ M. G. Tarzila,⁷⁸ A. Tauro,³⁶ G. Tejada Muñoz,² A. Telesca,³⁶ K. Terasaki,¹²⁷ C. Terrevoli,³⁰ B. Teyssier,¹³⁰ J. Thäder,⁷⁴ D. Thomas,¹¹⁸ R. Tieulent,¹³⁰ A. R. Timmins,¹²² A. Toia,⁵³ S. Trogolo,²⁷ G. Trombetta,³³ V. Trubnikov,³ W. H. Trzaska,¹²³ T. Tsuji,¹²⁷ A. Tumkin,⁹⁹ R. Turrisi,¹⁰⁷ T. S. Tveter,²² K. Ullaland,¹⁸ A. Uras,¹³⁰ G. L. Usai,²⁵ A. Utrobicic,¹²⁹ M. Vajzer,⁸⁴ M. Vala,⁵⁹ L. Valencia Palomo,⁷⁰ S. Vallero,²⁷ J. Van Der Maarel,⁵⁷ J. W. Van Hoorne,³⁶ M. van Leeuwen,⁵⁷ T. Vanat,⁸⁴ P. Vande Vyvre,³⁶ D. Varga,¹³⁵ A. Vargas,² M. Vargyas,¹²³ R. Varma,⁴⁸ M. Vasileiou,⁸⁹ A. Vasiliev,⁸⁰ A. Vauthier,⁷¹ V. Vechemin,¹³¹ A. M. Veen,⁵⁷ M. Veldhoen,⁵⁷ A. Velure,¹⁸ M. Venaruzzo,⁷³ E. Vercellin,²⁷ S. Vergara Limón,² R. Vernet,⁸ M. Verweij,¹³⁴ L. Vickovic,¹¹⁶ G. Viesti,^{30,†} J. Viinikainen,¹²³ Z. Vilakazi,¹²⁶ O. Villalobos Baillie,¹⁰¹ A. Villatoro Tello,² A. Vinogradov,⁸⁰ L. Vinogradov,¹³¹ Y. Vinogradov,^{99,†} T. Virgili,³¹ V. Vislavicius,³⁴ Y. P. Viyogi,¹³² A. Vodopyanov,⁶⁶ M. A. Völkl,⁹⁴ K. Voloshin,⁵⁸ S. A. Voloshin,¹³⁴ G. Volpe,¹³⁵ B. von Haller,³⁶ I. Vorobyev,^{37,93} D. Vranic,^{97,36} J. Vrláková,⁴¹ B. Vulpescu,⁷⁰ A. Vyushin,⁹⁹ B. Wagner,¹⁸ J. Wagner,⁹⁷ H. Wang,⁵⁷ M. Wang,^{7,113} D. Watanabe,¹²⁸ Y. Watanabe,¹²⁷ M. Weber,^{112,36} S. G. Weber,⁹⁷ D. F. Weiser,⁹⁴ J. P. Wessels,⁵⁴ U. Westerhoff,⁵⁴ A. M. Whitehead,⁹⁰ J. Wiechula,³⁵ J. Wikne,²² M. Wilde,⁵⁴ G. Wilk,⁷⁷ J. Wilkinson,⁹⁴ M. C. S. Williams,¹⁰⁴ B. Windelband,⁹⁴ M. Winn,⁹⁴ C. G. Yaldo,¹³⁴ H. Yang,⁵⁷ P. Yang,⁷ S. Yano,⁴⁷ C. Yasar,⁶⁹ Z. Yin,⁷ H. Yokoyama,¹²⁸ I.-K. Yoo,⁹⁶ J. H. Yoon,⁵⁰ V. Yurchenko,³ I. Yushmanov,⁸⁰ A. Zaborowska,¹³³ V. Zaccolo,⁸¹ A. Zaman,¹⁶ C. Zampolli,¹⁰⁴ H. J. C. Zanoli,¹²⁰ S. Zaporozhets,⁶⁶ N. Zardoshti,¹⁰¹ A. Zarochentsev,¹³¹ P. Závada,⁶⁰ N. Zaviyalov,⁹⁹ H. Zbroszczyk,¹³³ I. S. Zgura,⁶² M. Zhalov,⁸⁶ H. Zhang,¹⁸ X. Zhang,⁷⁴ Y. Zhang,⁷ C. Zhang,⁵⁷ Z. Zhang,⁷ C. Zhao,²² N. Zhigareva,⁵⁸ D. Zhou,⁷ Y. Zhou,⁸¹ Z. Zhou,¹⁸ H. Zhu,¹⁸ J. Zhu,^{113,7} A. Zichichi,^{28,12} A. Zimmermann,⁹⁴ M. B. Zimmermann,^{36,54} G. Zinovjev,³ and M. Zyzak⁴³

(ALICE Collaboration)

¹A. I. Alikhanyan National Science Laboratory (Yerevan Physics Institute) Foundation, Yerevan, Armenia²Benemérita Universidad Autónoma de Puebla, Puebla, Mexico³Bogolyubov Institute for Theoretical Physics, Kiev, Ukraine⁴Bose Institute, Department of Physics and Centre for Astroparticle Physics and Space Science (CAPSS), Kolkata, India⁵Budker Institute for Nuclear Physics, Novosibirsk, Russia⁶California Polytechnic State University, San Luis Obispo, California, USA⁷Central China Normal University, Wuhan, China⁸Centre de Calcul de l'IN2P3, Villeurbanne, France⁹Centro de Aplicaciones Tecnológicas y Desarrollo Nuclear (CEADEN), Havana, Cuba¹⁰Centro de Investigaciones Energéticas Medioambientales y Tecnológicas (CIEMAT), Madrid, Spain¹¹Centro de Investigación y de Estudios Avanzados (CINVESTAV), Mexico City and Mérida, Mexico¹²Centro Fermi—Museo Storico della Fisica e Centro Studi e Ricerche “Enrico Fermi,” Rome, Italy¹³Chicago State University, Chicago, Illinois, USA¹⁴China Institute of Atomic Energy, Beijing, China¹⁵Commissariat à l’Energie Atomique, IRFU, Saclay, France¹⁶COMSATS Institute of Information Technology (CIIT), Islamabad, Pakistan¹⁷Departamento de Física de Partículas and IGFAE, Universidad de Santiago de Compostela, Santiago de Compostela, Spain¹⁸Department of Physics and Technology, University of Bergen, Bergen, Norway¹⁹Department of Physics, Aligarh Muslim University, Aligarh, India²⁰Department of Physics, Ohio State University, Columbus, Ohio, USA²¹Department of Physics, Sejong University, Seoul, South Korea²²Department of Physics, University of Oslo, Oslo, Norway²³Dipartimento di Elettrotecnica ed Elettronica del Politecnico, Bari, Italy

- ²⁴*Dipartimento di Fisica dell'Università 'La Sapienza' and Sezione INFN, Rome, Italy*
- ²⁵*Dipartimento di Fisica dell'Università and Sezione INFN, Cagliari, Italy*
- ²⁶*Dipartimento di Fisica dell'Università and Sezione INFN, Trieste, Italy*
- ²⁷*Dipartimento di Fisica dell'Università and Sezione INFN, Turin, Italy*
- ²⁸*Dipartimento di Fisica e Astronomia dell'Università and Sezione INFN, Bologna, Italy*
- ²⁹*Dipartimento di Fisica e Astronomia dell'Università and Sezione INFN, Catania, Italy*
- ³⁰*Dipartimento di Fisica e Astronomia dell'Università and Sezione INFN, Padova, Italy*
- ³¹*Dipartimento di Fisica "E.R. Caianiello" dell'Università and Gruppo Collegato INFN, Salerno, Italy*
- ³²*Dipartimento di Scienze e Innovazione Tecnologica dell'Università del Piemonte Orientale and Gruppo Collegato INFN, Alessandria, Italy*
- ³³*Dipartimento Interateneo di Fisica "M. Merlin" and Sezione INFN, Bari, Italy*
- ³⁴*Division of Experimental High Energy Physics, University of Lund, Lund, Sweden*
- ³⁵*Eberhard Karls Universität Tübingen, Tübingen, Germany*
- ³⁶*European Organization for Nuclear Research (CERN), Geneva, Switzerland*
- ³⁷*Excellence Cluster Universe, Technische Universität München, Munich, Germany*
- ³⁸*Faculty of Engineering, Bergen University College, Bergen, Norway*
- ³⁹*Faculty of Mathematics, Physics and Informatics, Comenius University, Bratislava, Slovakia*
- ⁴⁰*Faculty of Nuclear Sciences and Physical Engineering, Czech Technical University in Prague, Prague, Czech Republic*
- ⁴¹*Faculty of Science, P.J. Šafárik University, Košice, Slovakia*
- ⁴²*Faculty of Technology, Buskerud and Vestfold University College, Vestfold, Norway*
- ⁴³*Frankfurt Institute for Advanced Studies, Johann Wolfgang Goethe-Universität Frankfurt, Frankfurt, Germany*
- ⁴⁴*Gangneung-Wonju National University, Gangneung, South Korea*
- ⁴⁵*Gauhati University, Department of Physics, Guwahati, India*
- ⁴⁶*Helsinki Institute of Physics (HIP), Helsinki, Finland*
- ⁴⁷*Hiroshima University, Hiroshima, Japan*
- ⁴⁸*Indian Institute of Technology Bombay (IIT), Mumbai, India*
- ⁴⁹*Indian Institute of Technology Indore, Indore (IITI), India*
- ⁵⁰*Inha University, Incheon, South Korea*
- ⁵¹*Institut de Physique Nucléaire d'Orsay (IPNO), Université Paris-Sud, CNRS-IN2P3, Orsay, France*
- ⁵²*Institut für Informatik, Johann Wolfgang Goethe-Universität Frankfurt, Frankfurt, Germany*
- ⁵³*Institut für Kernphysik, Johann Wolfgang Goethe-Universität Frankfurt, Frankfurt, Germany*
- ⁵⁴*Institut für Kernphysik, Westfälische Wilhelms-Universität Münster, Münster, Germany*
- ⁵⁵*Institut Pluridisciplinaire Hubert Curien (IPHC), Université de Strasbourg, CNRS-IN2P3, Strasbourg, France*
- ⁵⁶*Institute for Nuclear Research, Academy of Sciences, Moscow, Russia*
- ⁵⁷*Institute for Subatomic Physics of Utrecht University, Utrecht, Netherlands*
- ⁵⁸*Institute for Theoretical and Experimental Physics, Moscow, Russia*
- ⁵⁹*Institute of Experimental Physics, Slovak Academy of Sciences, Košice, Slovakia*
- ⁶⁰*Institute of Physics, Academy of Sciences of the Czech Republic, Prague, Czech Republic*
- ⁶¹*Institute of Physics, Bhubaneswar, India*
- ⁶²*Institute of Space Science (ISS), Bucharest, Romania*
- ⁶³*Instituto de Ciencias Nucleares, Universidad Nacional Autónoma de México, Mexico City, Mexico*
- ⁶⁴*Instituto de Física, Universidad Nacional Autónoma de México, Mexico City, Mexico*
- ⁶⁵*iThemba LABS, National Research Foundation, Somerset West, South Africa*
- ⁶⁶*Joint Institute for Nuclear Research (JINR), Dubna, Russia*
- ⁶⁷*Konkuk University, Seoul, South Korea*
- ⁶⁸*Korea Institute of Science and Technology Information, Daejeon, South Korea*
- ⁶⁹*KTO Karatay University, Konya, Turkey*
- ⁷⁰*Laboratoire de Physique Corpusculaire (LPC), Clermont Université, Université Blaise Pascal, CNRS-IN2P3, Clermont-Ferrand, France*
- ⁷¹*Laboratoire de Physique Subatomique et de Cosmologie, Université Grenoble-Alpes, CNRS-IN2P3, Grenoble, France*
- ⁷²*Laboratori Nazionali di Frascati, INFN, Frascati, Italy*
- ⁷³*Laboratori Nazionali di Legnaro, INFN, Legnaro, Italy*
- ⁷⁴*Lawrence Berkeley National Laboratory, Berkeley, California, USA*
- ⁷⁵*Moscow Engineering Physics Institute, Moscow, Russia*
- ⁷⁶*Nagasaki Institute of Applied Science, Nagasaki, Japan*
- ⁷⁷*National Centre for Nuclear Studies, Warsaw, Poland*
- ⁷⁸*National Institute for Physics and Nuclear Engineering, Bucharest, Romania*

- ⁷⁹National Institute of Science Education and Research, Bhubaneswar, India
⁸⁰National Research Centre Kurchatov Institute, Moscow, Russia
⁸¹Niels Bohr Institute, University of Copenhagen, Copenhagen, Denmark
⁸²Nikhef, Nationaal instituut voor subatomaire fysica, Amsterdam, Netherlands
⁸³Nuclear Physics Group, STFC Daresbury Laboratory, Daresbury, United Kingdom
⁸⁴Nuclear Physics Institute, Academy of Sciences of the Czech Republic, Řež u Prahy, Czech Republic
⁸⁵Oak Ridge National Laboratory, Oak Ridge, Tennessee, USA
⁸⁶Petersburg Nuclear Physics Institute, Gatchina, Russia
⁸⁷Physics Department, Creighton University, Omaha, Nebraska, USA
⁸⁸Physics Department, Panjab University, Chandigarh, India
⁸⁹Physics Department, University of Athens, Athens, Greece
⁹⁰Physics Department, University of Cape Town, Cape Town, South Africa
⁹¹Physics Department, University of Jammu, Jammu, India
⁹²Physics Department, University of Rajasthan, Jaipur, India
⁹³Physik Department, Technische Universität München, Munich, Germany
⁹⁴Physikalisches Institut, Ruprecht-Karls-Universität Heidelberg, Heidelberg, Germany
⁹⁵Purdue University, West Lafayette, Indiana, USA
⁹⁶Pusan National University, Pusan, South Korea
⁹⁷Research Division and ExtreMe Matter Institute EMMI, GSI Helmholtzzentrum für Schwerionenforschung, Darmstadt, Germany
⁹⁸Rudjer Bošković Institute, Zagreb, Croatia
⁹⁹Russian Federal Nuclear Center (VNIIEF), Sarov, Russia
¹⁰⁰Saha Institute of Nuclear Physics, Kolkata, India
¹⁰¹School of Physics and Astronomy, University of Birmingham, Birmingham, United Kingdom
¹⁰²Sección Física, Departamento de Ciencias, Pontificia Universidad Católica del Perú, Lima, Peru
¹⁰³Sezione INFN, Bari, Italy
¹⁰⁴Sezione INFN, Bologna, Italy
¹⁰⁵Sezione INFN, Cagliari, Italy
¹⁰⁶Sezione INFN, Catania, Italy
¹⁰⁷Sezione INFN, Padova, Italy
¹⁰⁸Sezione INFN, Rome, Italy
¹⁰⁹Sezione INFN, Trieste, Italy
¹¹⁰Sezione INFN, Turin, Italy
¹¹¹SSC IHEP of NRC Kurchatov institute, Protvino, Russia
¹¹²Stefan Meyer Institut für Subatomare Physik (SMI), Vienna, Austria
¹¹³SUBATECH, Ecole des Mines de Nantes, Université de Nantes, CNRS-IN2P3, Nantes, France
¹¹⁴Suranaree University of Technology, Nakhon Ratchasima, Thailand
¹¹⁵Technical University of Košice, Košice, Slovakia
¹¹⁶Technical University of Split FESB, Split, Croatia
¹¹⁷The Henryk Niewodniczanski Institute of Nuclear Physics, Polish Academy of Sciences, Cracow, Poland
¹¹⁸The University of Texas at Austin, Physics Department, Austin, Texas, USA
¹¹⁹Universidad Autónoma de Sinaloa, Culiacán, Mexico
¹²⁰Universidade de São Paulo (USP), São Paulo, Brazil
¹²¹Universidade Estadual de Campinas (UNICAMP), Campinas, Brazil
¹²²University of Houston, Houston, Texas, USA
¹²³University of Jyväskylä, Jyväskylä, Finland
¹²⁴University of Liverpool, Liverpool, United Kingdom
¹²⁵University of Tennessee, Knoxville, Tennessee, USA
¹²⁶University of the Witwatersrand, Johannesburg, South Africa
¹²⁷University of Tokyo, Tokyo, Japan
¹²⁸University of Tsukuba, Tsukuba, Japan
¹²⁹University of Zagreb, Zagreb, Croatia
¹³⁰Université de Lyon, Université Lyon 1, CNRS/IN2P3, IPN-Lyon, Villeurbanne, France
¹³¹V. Fock Institute for Physics, St. Petersburg State University, St. Petersburg, Russia
¹³²Variable Energy Cyclotron Centre, Kolkata, India
¹³³Warsaw University of Technology, Warsaw, Poland
¹³⁴Wayne State University, Detroit, Michigan, USA
¹³⁵Wigner Research Centre for Physics, Hungarian Academy of Sciences, Budapest, Hungary
¹³⁶Yale University, New Haven, Connecticut, USA
¹³⁷Yonsei University, Seoul, South Korea

¹³⁸*Zentrum für Technologietransfer und Telekommunikation (ZTT), Fachhochschule Worms,
Worms, Germany*

[†]Deceased.

^aAlso at Georgia State University, Atlanta, Georgia, USA.

^bAlso at Department of Applied Physics, Aligarh Muslim University, Aligarh, India.

^cAlso at M.V. Lomonosov Moscow State University, D.V. Skobeltsyn Institute of Nuclear, Physics, Moscow, Russia.